

Damage detection in structures using robust baseline models

Jhonatan Camacho-Navarro^{*†}, Magda Ruiz^{*}, Rodolfo Villamizar[†], Luis Mujica^{*}, Fernando Martínez^{††}

^{*}Department of Applied Mathematics III, Escola Universitària d'Enginyeria Tècnica Industrial de Barcelona (EUETIB), Universitat Politècnica de Catalunya (UPC) BARCELONATECH, Comte d'Urgell 187, E-08036, Barcelona, Spain

jhonatan.camacho@estudiant.upc.edu, magda.ruiz@upc.edu, luis.eduardo.mujica@upc.edu,

[†]Escuela de Ingenierías Eléctrica, Electrónica y de Telecomunicaciones (E3T), Universidad Industrial de Santander (UIS). Grupo de Control Electrónica Modelado y Simulación (CEMOS). Santander, Colombia. rovillam@uis.edu.co

^{††} Department of sensors, Ikerlan Research Center, Spains
fmartinez@ikerlan.es

Key words: Piezo-diagnostics, principal component analysis, time feature extraction, pipe leak damage detection, crack detection in a laboratory tower.

Summary: *This work deals with a previously proposed piezo-diagnostic methodology based on principal component analysis for structural damage detection. Previous works have demonstrated the effectiveness of baseline models to distinguish between structural damage and undamaged conditions, however, its robustness and reproducibility depends on a proper estimation of the principal components from undamaged data matrix measurements. Principal components are highly sensitive to the algorithm parameters used to compute the singular value decomposition, on the number of experiments collected for building the baseline model and on atypical measurements. In this work, the above conditions are studied by including a pre-processing state using time feature extraction in order to solve the ill-conditioned statistical problem due to the low ratio between undamaged cases and time piezo-electrical samples used for building the baseline model. In addition, a comparison between two methods (Proper Orthogonal Decomposition Vs NIPALS) used to estimate the principal components is done. Average of several experiments is computed to deal with atypical data cases and experimental results are obtained from two structures: i.) a carbon steel pipe section and ii.) a laboratory tower that mimics a wind turbine. Finally, damages are conditioned in order to produce leaks in the pipe section and a crack in one element of the laboratory tower.*

1 INTRODUCTION

The high sensitivity of the guided-wave ultrasonic technique has been an advantage for structural health monitoring applications [1]. Guided waves have been extensively studied for damage detection and characterization in a wide range of industrial applications, including transportation and civil engineering [2]. In this sense, it has been demonstrated that guided waves can be easily generated by using Lead Zirconate Titanate piezoelectric devices (PZT).

Thus, several researches have shown the feasibility of using PZT measurements for condition monitoring [3, 4, 5].

Singular value decomposition (SVD) is a common procedure to characterize ultrasonic elastic waves propagating into a medium. From this technique damage-sensitive orthogonal features are extracted to differentiate between damage and undamaged states. Several applications have demonstrated its robustness, for example by detecting saw cuts and fatigue cracks on aluminum beams [6] and mass scatterer detection in a hot water piping system in continuous operation [7], under variable environmental and operational conditions. However, this technique consumes high computing resources and requires especial treatment when processing big data matrices.

Thus, in this paper a comparison of three algorithms used to compute orthogonal features from experimental piezoelectric pitch–catch records are studied. These orthogonal features serve to represent a structural baseline model, which is a mean to obtain structural signature in presence or absence of damages. In addition, a preprocessing stage based on time-features extraction, from the recorded signals, is achieved to treat the influence of high dimensionality and low rank statistical problems. The efficacy of the implemented data driven approach is validated using experimental measurements from a steel carbon pipe section and a laboratory tower. It is demonstrated that detection of structural leaks and cracks is possible for the studied cases.

2 STRUCTURAL DAMAGE DETECTION ALGORITHM: PIEZO-DIAGNOSTICS BASED ON STATISTICAL INDEXES

Figure 1 summarizes the general proposed scheme of the piezo-diagnostics approach for structural leaks and cracks detection. The effectiveness of this methodology has been previously validated for damage detection in aluminum plates, composite structures, aircraft sections and pipework structures [8, 9, 10].

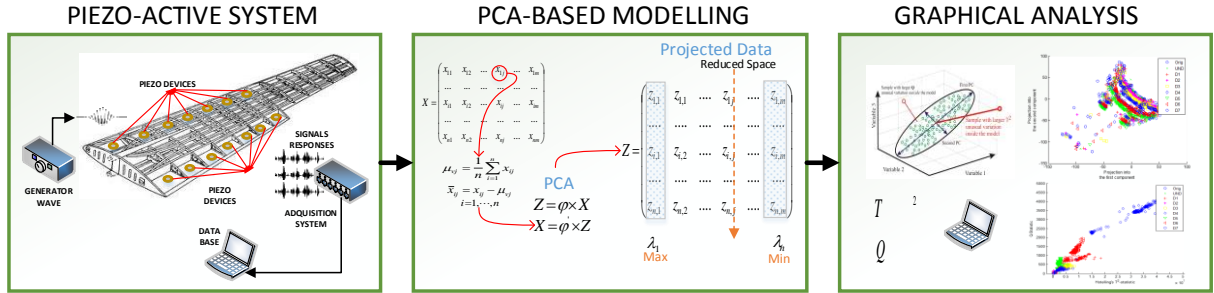


Figure 1: Piezo-diagnostic approach for structural damage identification.

According to Figure 1, in the piezo-diagnostic approach one or a net of piezo-ceramic sensors are used to record elastic wave signals induced by a piezo-actuator. The conceptual steps involved for damage detection based on piezo-diagnostic approach are [8]:

- i. Collect signals obtained from the pristine condition of the structure (baseline signals) in order to arrange a matrix of undamaged records:

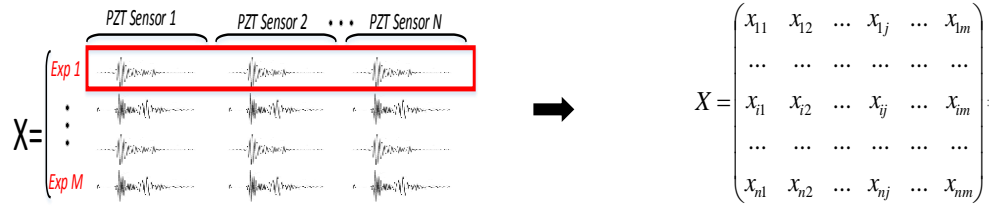


Figure 2: Undamaged baseline matrix

- ii. Where, M experiment repetitions are conducted for the healthy reference in order to consider measurement noise in the baseline records. Therefore, the signals from N PZT sensors are unfolded in the undamaged baseline matrix.
- iii. Apply Group-Scaling normalization procedure to eliminate bias and scale variance in the undamaged baseline matrix. Each data-point x_{ij} is scaled by considering changes between sensors. The standardization is computed by using the mean of each time sample for every experiment and the standard deviation of each sensor sample vector.
- iv. Decompose the normalized undamaged baseline matrix \bar{X} into a model part and a noise part:

$$\bar{X} = ZP^T + E = \text{model} + \text{noise} \quad (1)$$

The model ZP^T in (1) corresponds to a new reduced space of coordinates with minimal redundancy, based on the variance–covariance of the original data. P is a linear transformation matrix that relates the data matrix \bar{X} in the new coordinates. P denotes the principal components and Z the projected matrix to the reduced space. The noise E-matrix is the part of \bar{X} , which is not explained by ZP^T and describes the residual variance neglected by the statistical model. The available methods to determine the P matrix will be detailed in the next section.

- v. Validate the statistical model (1) with new PZT measurements representing the current state of the structure. These measurements are organized in a row vector as it is highlighted in Figure 2. This row vector is standardized by applying GroupScaling and considering mean values and standard deviations of the undamaged baseline matrix. Then, the normalized row vector of new measurements is projected onto the reduced space by using the statistical model (1). Differences between baseline model and current state are attributed to damage.

INDICES FOR FAULT DIAGNOSIS

The above piezo-diagnostic approach corresponds to conventional data-driven SHM methods based only on measurement analysis. The structural damage detection is achieved by differentiating one or more features between the sets of the processed signals. For this purpose, two common indexes used in fault diagnosis systems are computed: Hotelling t-square and Q-statistics.

The Q-statistic is a lack of fit measure between the analyzed experiment and the statistical model (2):

$$Q = \sum_j (e_j)^2 \quad (2)$$

Where, e_j is the residual error for each j – th principal component used to reconstruct the experiment signal.

The Hotelling T^2 statistic indicates how far each measurement is from the center (scores = 0) of the model:

$$T^2 = Z' \lambda^{-1} Z \quad (3)$$

Where, λ are the respective variances within the model.

Q and T^2 statistics are used to detect abnormal behavior of guided wave signals traveling into the structure compared to the baseline model.

3 TRANSFORMATION MATRIX OBTAINING METHODS

Principal Component Analysis (PCA) provides a simple way to emphasize relationships among patterns. Thus, by using PCA it is possible describe changes of elements in a data-matrix by mean of a model expressed by (1). Several interpretations of PCA are presented in the literature: Karhunen-Loève decomposition (KLV), Proper Orthogonal Decomposition (POD) and Singular Value Decomposition (SVD) and in general, it is used to extract dominant features from experimental data. Liang et al [11] describe the equivalence of the different PCA interpretations.

Common methods for obtaining the PCA transformation matrix are detailed in this section in order to use them in the undamaged baseline matrix processing. It is remarked that dimensions of dataset matrix in Figure 2 correspond to $n \ll m$. In this case, n are the experiment repetitions (< 200), while m depends of the sample frequency, time length records and the number of PZT sensors (> 20.000).

3.1 Classical procedure

The classical algorithm to obtain the PCA matrix transformation consists of three main steps:

- I. Estimate the covariance matrix of the normalized data-matrix \bar{X} :

$$C_{\bar{x}} = \frac{1}{n-1} (\bar{X})(\bar{X})^T \quad (4)$$

- II. Calculate the Eigenvectors-Eigenvalues of the covariance matrix.
- III. Select the first eigenvectors as the principal components. The transformation matrix P contains column vectors of the selected eigenvectors, while the model variance is described by the respective eigenvalues.

For obtaining, the Eigenvectors-Eigenvalues of the step II.) it is necessary to compute the singular value decomposition, where an Eigenvector is a nonzero vector that satisfies the equation (5):

$$A\vec{v} = \lambda\vec{v} \quad (5)$$

Where, A is a square matrix, λ is a scalar, and \vec{v} is the eigenvector. The eigenvalues and

eigenvectors can be found by solving a matrix as a linear equations system.

For the case of data in Figure 2 the covariance matrix is $m \times m$, thus it is necessary to determine m eigenvectors and eigenvalues. However, because $n \ll m$ only $n-1$ eigenvalues are nonzero, the transformation matrix P consists of $n-1$ statistically significant principal components. The QR algorithm [12] is commonly used to obtain the singular value decomposition of a data-matrix expressed in (5).

3.2 Alternative methods

Since only $n - 1$ eigenvalues are nonzero, alternative methods can be used to estimate the singular value decomposition of a data-matrix. These methods are intended to minimize the computational cost, taking advantage of the property $n \ll m$.

Proper Orthogonal decomposition (POD)

Proper orthogonal decomposition method allows describing a process by a low-dimensioned model represented by a set of base functions, obtained from the dynamic response. POD is based on the singular value decomposition for non-square matrix and recently, it has been used for damage detection in structures [13]. By applying POD, the normalized undamaged baseline matrix can be decomposed by (6):

$$\bar{X} = U\Sigma V^T \quad (6)$$

Where, U and V are called the left-singular vectors and right-singular vectors of \bar{X} , respectively and Σ is a diagonal matrix with the nonzero singular values. If the left-singular vectors of \bar{X} are eigenvectors of $\bar{X}\bar{X}^T$ and the right-singular vectors of \bar{X} are eigenvectors of $\bar{X}^T\bar{X}$, it is possible to establish that:

$$\begin{aligned} \bar{X}\bar{X}^T &= (U\Sigma V^T)(U\Sigma V^T)^T = U\Sigma V^T V \Sigma^T U^T = U\Sigma^2 U^T \\ \bar{X}^T\bar{X} &= (U\Sigma V^T)^T(U\Sigma V^T) = V\Sigma^T U^T U \Sigma V^T = V\Sigma^2 V^T \end{aligned} \quad (7)$$

According to classical procedure, the transformation matrix P corresponds to the singular value decomposition of $\bar{X}\bar{X}^T$, thus it can be inferred from (7) that $U = P$. By using (6), the transformation matrix can be computed as:

$$P \equiv \bar{X}\Sigma^{-1}V \quad (8)$$

In addition, it is noted that the non-zero singular values of \bar{X} are equal the square roots of the non-zero eigenvalues of both $\bar{X}\bar{X}^T$ and $\bar{X}^T\bar{X}$. In this sense, it is enough to find the singular value decomposition of $\bar{X}^T\bar{X}$, with dimensions $n \times n$ instead of $\bar{X}\bar{X}^T$ with dimensions $m \times m$. These relations reduce the computational cost required to compute the transformation matrix of the statistical model (1).

Non-linear Iterative Partial Least Squares (NIPALS)

NIPALS algorithm is one of the methods used to compute eigenvectors, where Figure 3 presents an overview of this algorithm.

Iterations (i=1 to number-of-PCs):

1. Project X onto t to find the corresponding loading p
 $p = (E_{(i-1)}^T t) / (t^T t)$
2. Normalise loading vector p to length 1
 $p = p * (p^T p)^{-0.5}$
3. Project X onto p to find corresponding score vector t
 $t = (E_{(i-1)} p) / (p^T p)$
4. Check for convergence. If difference between eigenvalues $\tau_{new} = (t^T t)$ and τ_{old} (from last iteration) is larger than $threshold * \tau_{new}$ return to step 1.
5. Remove the estimated PC component from $E_{(i-1)}$
 $E_{(i)} = E_{(i-1)} - (t p^T)$

Figure 3: NIPALS algorithm pseudo-code [14]

4 TIME FEATURES EXTRACTION STAGE FOR DAMAGE DETECTIONS

Since the statistical problem for PCA modeling is ill conditioned because the covariance matrix is estimated with less samples than variables is necessary to evaluate its influence. Thus, in this work a time features extraction procedure is applied by building a new baseline undamaged matrix with the next PZT time signals additional features: root mean squared value, maximum value, mean value and standard deviation. Then, the statistical model is obtained from this new feature matrix, which satisfies the condition $n > m$.

In addition, an alternative preprocessing stage based on cross correlation analysis is explored in order to improve the damage discrimination, by excluding external signals common to actuation and sensing elements, and to eliminate noisy data trends. Thus, cross-correlation between actuation and sensing piezo-signals is computed, before the PCA analysis. The cross-correlation function between two signals $X(t)$ and $Y(t)$ is defined by (9).

$$R_{XY}(t, t + \tau) = \lim_{N \rightarrow \infty} \frac{1}{N} \sum_{k=1}^N X_k(t) Y_k(t + \tau), \quad (9)$$

where N is the number of samples and τ is the lag time interval used to compute the cross-correlation function. Then, the statistical model is obtained from a cross-correlated PZT signals baseline matrix.

5 EXPERIMENTAL RESULTS

Two experiments were conducted on two structural lab models in order to evaluate the proposed methodology. The first experiment corresponds to detect leaks in a carbon steel pipe section and the second one corresponds to detect crack in a laboratory tower. First, the three above mentioned algorithms used to compute the transformation matrix were evaluated by using experimental data from the pipe section. Then, the best algorithm was used to detect cracks in the laboratory tower

5.1 Excitation signal

In order to induce guided waves into the test structures a burst type signal (Figure 4), generated by means of an AWG PicoScope series 2000, was used to excite the PZT actuator around its resonance frequency (~ 100 KHz, Figure 5) and then it is amplified to ± 10 V.

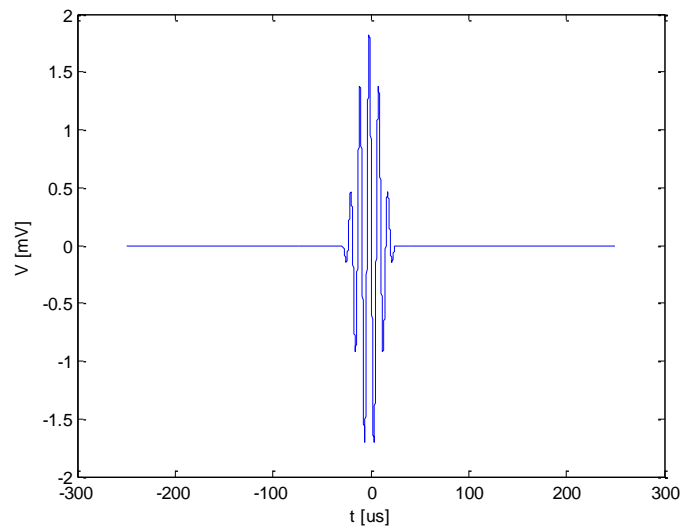


Figure 4: Burst type excitation before amplification.

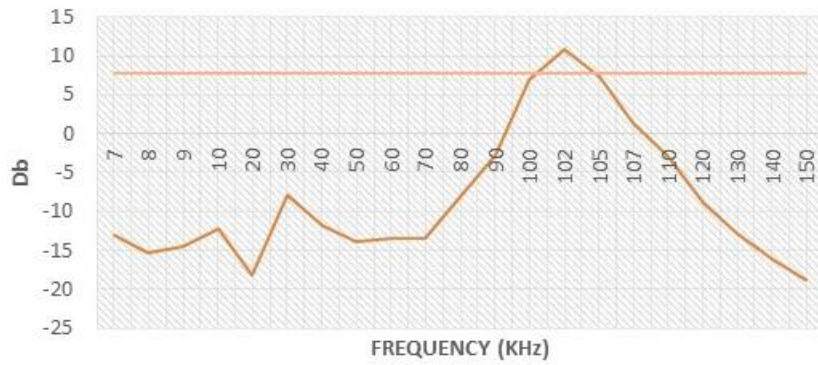


Figure 5: PZT frequency response

5.2 Carbon steel pipe section

The first specimen used as test structure is a carbon-steel pipe section of dimensions 100x 2.54 x0.3 cm (length, diameter, thickness). The pipe section contains bridles at its ends and a valve that controls the airflow from a compressor at 80 psi (Figure 6). Four piezoelectric devices (PZT) were attached along the structure as sensors, while another one is attached as actuator.

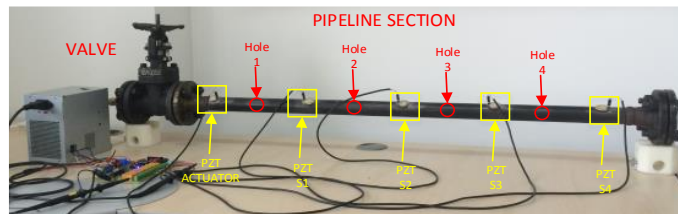


Figure 6: Experiment configuration

In order to induce leaks in the test structure, four 1/4-inch holes were drilled along the pipe section wall with adjustable screws. Table 1 details the leaks combination experimented in this work, where for each one 100-experiment repetitions were conducted during 1s of periodic excitation signal (undamaged case is labeled ‘UND’).

Label	Holes (Red=open)	Label	Holes (Red=open)
D1	H1,H2,H3,H4	D5	H1,H2,H3,H4
D2	H1,H2,H3,H4	D6	H1,H2,H3,H2
D3	H1,H2,H3,H4	D7	H1,H2,H3,H4
D4	H1,H2,H3,H4		

Table 1: Leaks combination

The principal components were computed by using NIPALS, QR, and POD algorithms, where the first and second ones are depicted in Figure 7, after cross-correlation analysis is applied.

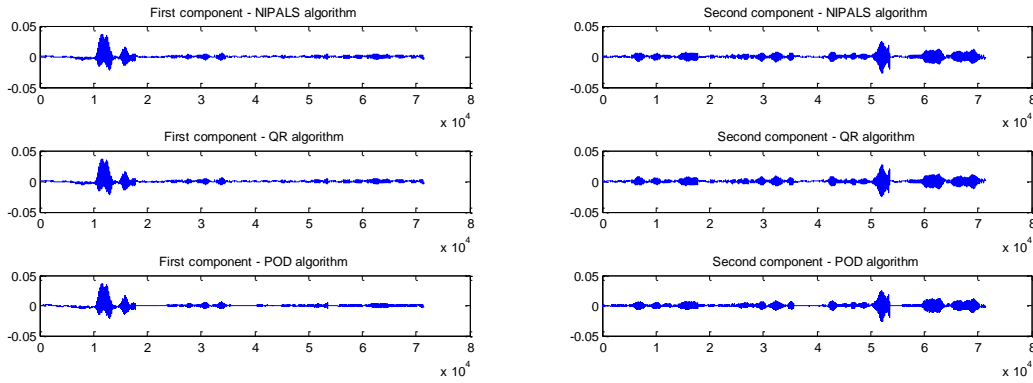


Figure 7: First and second principal components computed by using different algorithms

The processed matrix have dimensions 100×71444 , where the time required to compute all the 99 principal components for each algorithm are summarized in Table 2. The algorithms were executed in a PC with processor Intel(R) Core(TM) i7-4600U, CPU 2.70 GHz, and 8.0 GB RAM. According to Figure 7, no meaning visual differences are observed for the first two principal components.

Method	Time (s)
NIPALS	312.2113
QR	6.4468
POD	1.2624

Table 2: Time consuming for computing matrix transformation.

According to Table 2, minimum time is required for POD algorithm and maximum is for NIPALS. The time for POD algorithm is lower because a small size transpose matrix is processed, while NIPALS algorithm requires maximum 1000 iterations to find each component. In addition, for NIPALS algorithm a convergence failure is presented for components 19, 61, and 96 with a tolerance value of $1e-4$. The root mean squared error for all principal components are depicted in Figure 8.

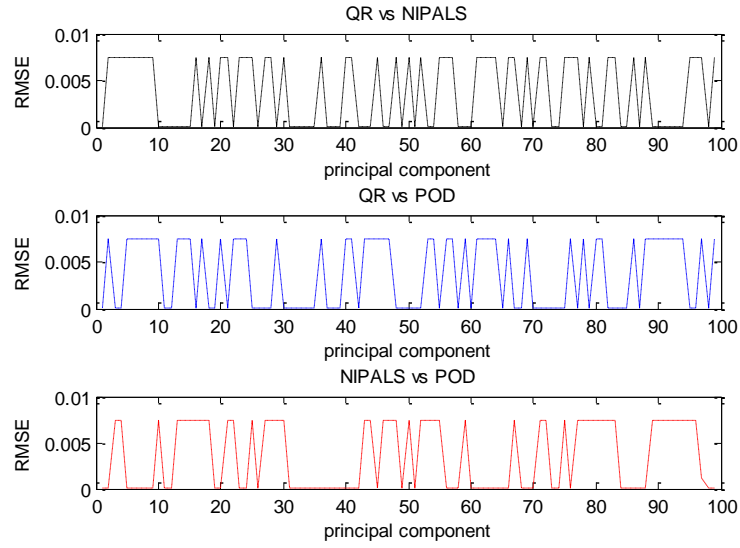


Figure 8: Root Mean Squared Error for each principal component

The non-normalized variances of the model obtained by means of NIPALS, QR and POD algorithms are presented in Figure 9a, while Figure 9b presents the variances normalized by its maximum value, in order to facilitate a comparison.

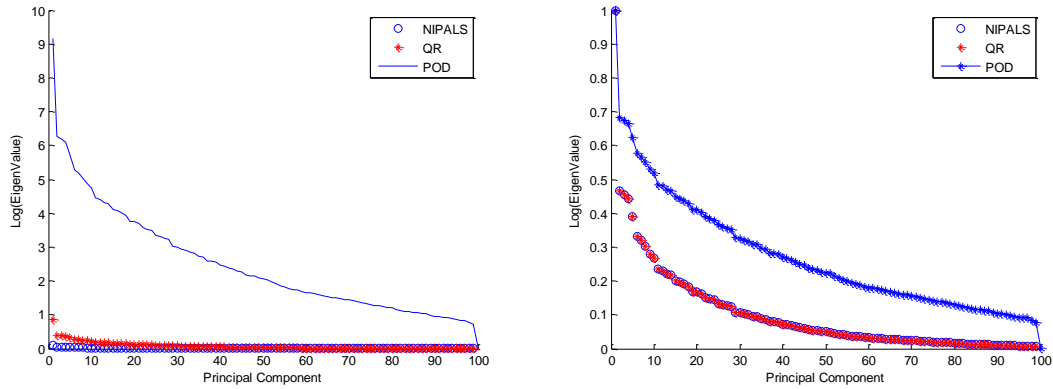


Figure 9: Model variances. Left: Original variances. Right: Normalized variances.

According to Figure 9b, the variances computed by using NIPALS and QR algorithms have the same trend in a different scale, but those computed by POD despite to describe similar trends an error is presented.

The evolution of the first and second component for the different leaks combination, computed by using POD, NIPALS and QR algorithms, are depicted in Figure 10. It is observed that the evolution of the scores computed by means of POD and NIPALS algorithms are very similar, while those computed by means of QR have similar trends in opposite direction.

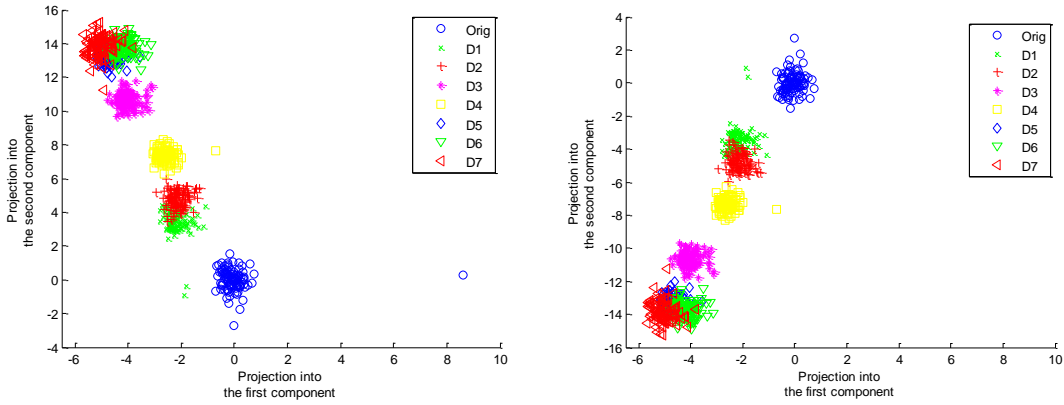


Figure 10: Graphical of two first scores for leak damages computed by: Left: QR algorithm. Right: NIPALS and POD algorithms

The Q and T^2 statistical indices are shown in Figure 11. It is observed a well defined separation for different leaks combinations, thus it can be concluded that the error presented in the estimation of principal components, for any of the three algorithms, do not affect the calculation of T^2 and Q statistical indexes. Also, the principal component directions do not influence on the statistical indices computation because their squared nature. Therefore, for this experimental case, this low error is imperceptible and clear boundaries can be identified by using any of the three studied algorithms.

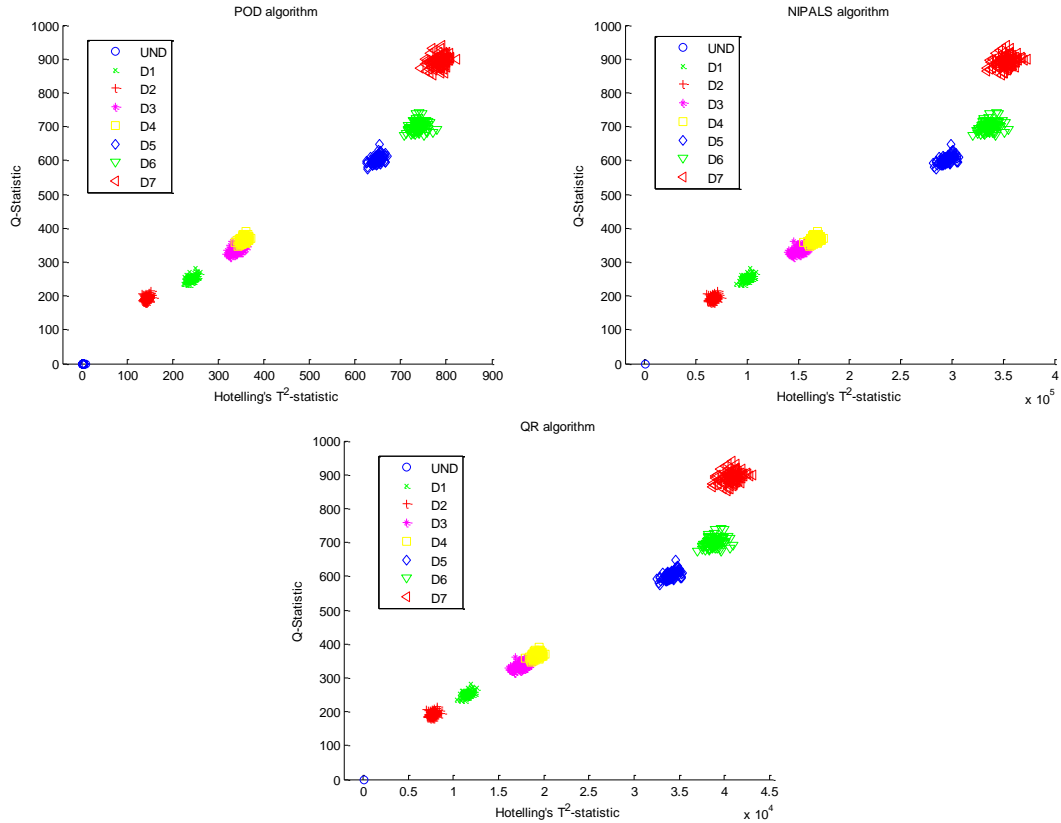


Figure 11: Statistical indexes for leak damage detection

Figure 12 presents experimental results by applying the preprocessing stage based on time features and the QR algorithm. It can be observed that better boundaries for leak damages are

obtained when the statistical model is computed with cross-correlated signals instead of using time features.

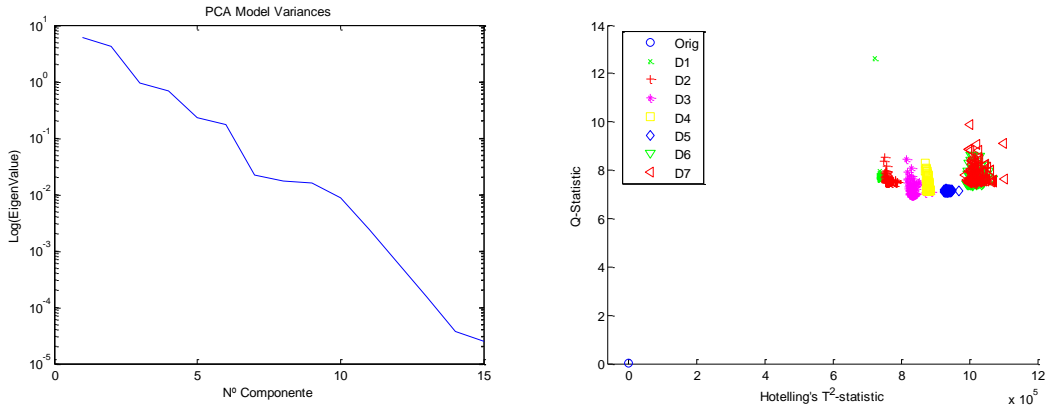


Figure 12: Damage identification by means of time features

5.3 Laboratory tower

The second test structure is a tower model, representing a wind turbine model previously studied for damage detection [15]. The structure (2.7 m high) is composed by three components (Figure 13a): jacket, tower and nacelle. A modal shaker simulates the nacelle mass and it is used to produce external 100 Hz white noise in the structure, which mimic the modal dynamics of an offshore wind turbine. Damage in the tower was induced by replacing one of the undamaged section in the jacket with a 5 mm cracked section (Figure 13b). Five PZT sensors were installed in the jacket (Figure 13a, red markers correspond to PZT devices) in order to record 50-experiment repetitions from guided wave structural responses produced by the PZT actuator.

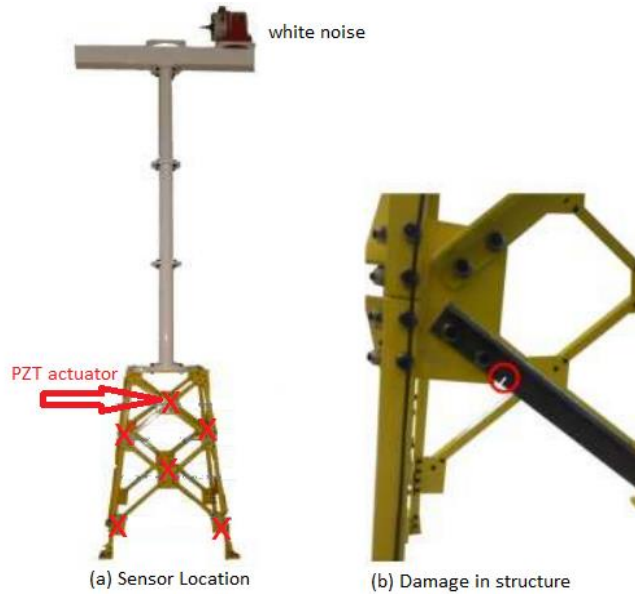


Figure 13: Laboratory tower structure.

Figure 14 presents the piezo-electrical response obtained from one of the PZT sensors by using a sample time $T_s = 32.0$ [ns]. It is observed a noise trend due to the modal shaker, which is removed by means of a digital filter (Figure 15).

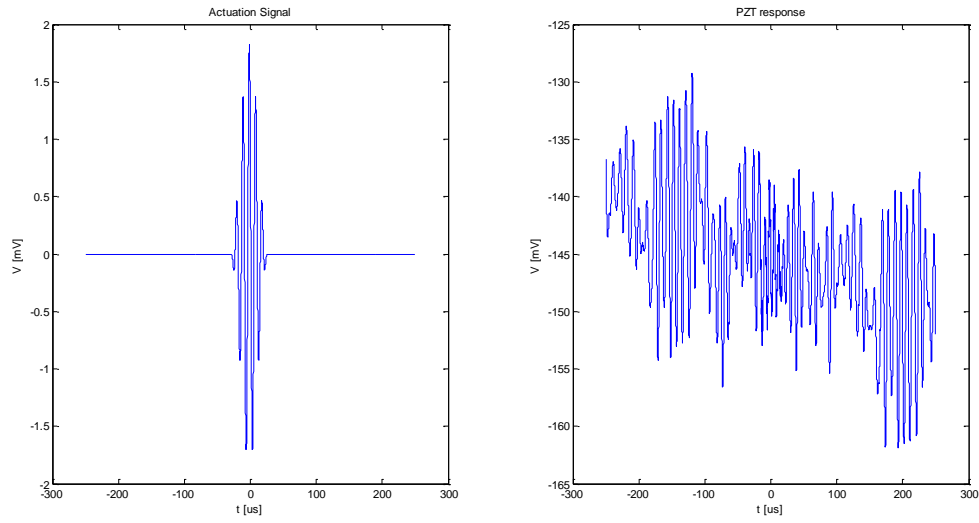


Figure 14: PZT response. Left: Actuator signal before amplification. Right: PZT Sensor measurement

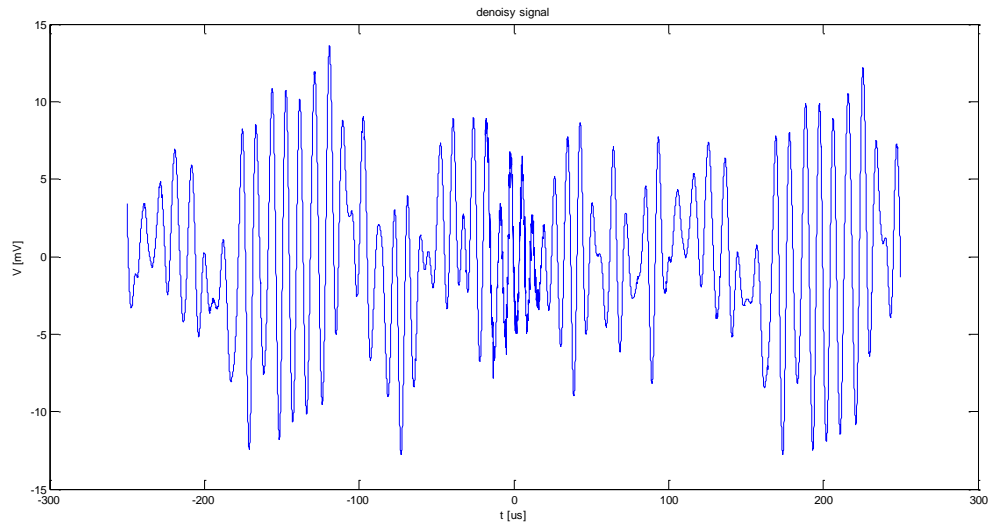


Figure 15: Noise removing from PZT response

Figure 16 depicts the model variances obtained by means of QR algorithm after processing the undamaged baseline matrix (50x156285).

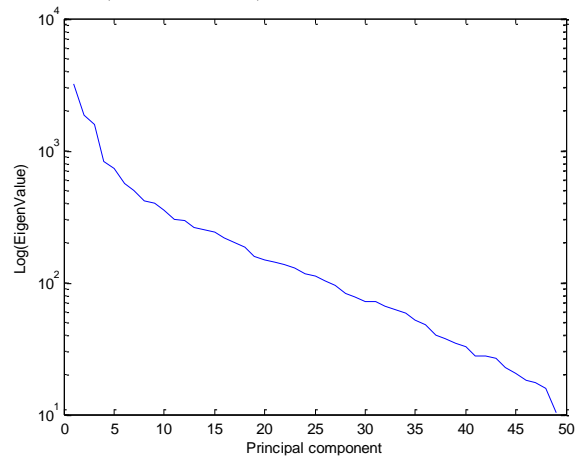


Figure 16: Statistical model variances.

Figure 17 presents the Q and T^2 statistical indexes for structural crack detection. It is observed meaning differences regarding to the undamaged state and a low dispersion for all experiments.

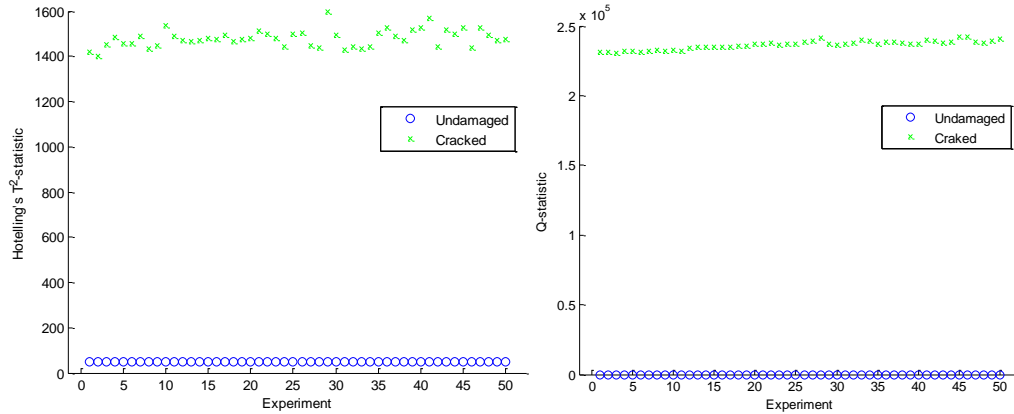


Figure 17: Statistical indexes for structural crack detection

6 CONCLUSIONS

The experimental results of the proposed algorithm based on PCA model shows capability for discriminate structural cracks and leaks. Three different algorithms to compute the transformation matrix were experimentally validated with no meaning differences to discern structural damages. Therefore, any of the algorithms can be implemented for damage detection purposes.

The low time computing resources, without convergence failures, reported when POD algorithm is applied, shows its suitability for implementing embedded codes. Additional features as memory usage and real-time performance should be studied in order to select a proper algorithm for continuous condition monitoring.

The robustness of PCA modelling to the ill-conditioned statistical problem was experimentally demonstrated for structural crack and leaks detection cases. However, a more extent experimentation is required in order to determine a minimum number of experiments to build the statistical model.

7 ACKNOWLEDGEMENT

This work has been developed as part of the research project: “Monitorización y Detección de Defectos en Estructuras usando Algoritmos Expertos Embebidos”, financed by the Departamento Administrativo de Ciencia y Tecnología Francisco José de Caldas – COLCIENCIAS and Banca Mundial in the Universidad Industrial de Santander, Colombia. Agosto 2012-Junio 2015.

REFERENCES

- [1] Raghavan, A., & Cesnik, C. E. (2007). Review of guided-wave structural health monitoring. *Shock and Vibration Digest*, 39(2), 91-116

- [2] Staszewski, W. J. (2004). Structural health monitoring using guided ultrasonic waves. In *Advances in smart technologies in structural engineering* (pp. 117-162). Springer Berlin Heidelberg.
- [3] Kabeya III, K. (1998). Structural health monitoring using multiple piezoelectric sensors and actuators.
- [4] Duan, W. H., Wang, Q., & Quek, S. T. (2010). Applications of piezoelectric materials in structural health monitoring and repair: Selected research examples. *Materials*, 3(12), 5169-5194.
- [5] Holnicki-Szulc, J., Kolakowski, P., Orlowska, A., Swiercz, A., Wiacek, D., and Zielinski, T. Piezodiagnostics – a new shm method and its potential engineering applications. Institute of Fundamental Technological Research, SMART-TECH Centre, Warsaw, Poland. *Mechanics of 21st Century - ICTAM04 Proceedings. XXI ICTAM*, 15-21 August 2004, Warsaw, Poland.
- [6] Vanlanduit, S., Parloo, E., & Guillaume, P. (2004). A robust singular value decomposition to detect damage under changing operation conditions and structural uncertainties. *Proceedings of IMAC-XXII*, Dearborn, Michigan, USA.
- [7] Liu, C., Harley, J. B., Bergés, M., Greve, D. W., & Oppenheim, I. J. (2015). Robust ultrasonic damage detection under complex environmental conditions using singular value decomposition. *Ultrasonics*.
- [8] Mujica, L. E., Rodellar, J., Fernandez, A., & Guemes, A. (2010). Q-statistic and T2-statistic PCA-based measures for damage assessment in structures. *Structural Health Monitoring*, 1475921710388972.
- [9] Tibaduiza Burgos, D. A., Mujica Delgado, L. E., Güemes Gordo, A., & Rodellar Benedé, J. (2010). Active piezoelectric system using PCA.
- [10] Torres-Arredondo, M. A., Buethe, I., Tibaduiza, D. A., Rodellar, J., & Fritzen, C. P. (2013). Damage detection and classification in pipework using acousto-ultrasonics and non-linear data-driven modelling. *Journal of Civil Structural Health Monitoring*, 3(4), 297-306.
- [11] Liang, Y. C., Lee, H. P., Lim, S. P., Lin, W. Z., Lee, K. H., & Wu, C. G. (2002). Proper orthogonal decomposition and its applications—Part I: Theory. *Journal of Sound and vibration*, 252(3), 527-544.
- [12] Wilkinson, J. H. (1965). *The algebraic eigenvalue problem* (Vol. 87). Oxford: Clarendon Press.
- [13] Shane, C., & Jha, R. (2011). Proper orthogonal decomposition based algorithm for detecting damage location and severity in composite beams. *Mechanical Systems and Signal Processing*, 25(3), 1062-1072.
- [14] Risvik, H. (2007). *Principal component analysis (PCA) & NIPALS algorithm*.
- [15] Zugasti, E., Mujica, L. E., Anduaga, J., & Martinez, F. (2013). Feature selection-Extraction methods based on PCA and mutual information to improve damage detection problem in offshore wind turbines. *Key Engineering Materials*, 569, 620-627.